A converged ubiquitin-proteasome pathway for the degradation of TOC and TOM tail-anchored receptors

Authors: Meijing Yang[1,3,†], Shuai Chen[2,†,&], Shey-Li Lim[1], Lang Yang[1,3], Jia Yi Zhong[1], Koon Chuen Chan[1], Zhizhu Zhao[1], Kam-Bo Wong[2,5], Junqi Wang[3,] and Boon Leong Lim[1,4,5,*]

Affiliations:

[1]School of Biological Sciences, University of Hong Kong; Pokfulam, Hong Kong, China.

[2]School of Life Sciences, the Chinese University of Hong Kong; Shatin, Hong Kong, China.

[3]Department of Biology, Southern University of Science and Technology; Shenzhen, China.

[4]HKU Shenzhen Institute of Research and Innovation; Shenzhen, China.

[5]State Key Laboratory of Agrobiotechnology; The Chinese University of Hong Kong, Hong Kong, China.

[†]These authors contributed equally to this work.

[*]Correspondence to: Boon Leong Lim (bllim@hku.hk)

Tel: 852-22990826

Fax: 852-25599114

[&]Present address: Marshall Laboratory of Biomedical Engineering, International Cancer Center, Laboratory of Evolutionary Theranostics (LET), School of Biomedical Engineering, Shenzhen University Medical School, Shenzhen University, Shenzhen, 518055, China.

Running title: Degradation pathways of TOC/TOM translocons

ABSTRACT

In plants, thousands of nucleus-encoded proteins translated in the cytosol are sorted to chloroplasts and mitochondria by binding to specific receptors of the TOC (translocon at the outer membranes of chloroplasts) and the TOM (translocon at the outer membranes of mitochondria) complexes for import into those organelles. The degradation pathways for these receptors are unclear. Here, we discovered a converged ubiquitin-proteasome pathway for the degradation of *Arabidopsis thaliana* TOC and TOM tail-anchored receptors. The receptors are ubiquitinated by E3 ligase(s) and pulled from the outer membranes by the AAA^+ ATPase CDC48, after which a previously characterized cytosolic protein, TTOP, binds to the exposed transmembrane domains (TMDs) at the C termini of the receptors and CDC48, and delivers these complexes to the 26S proteasome.

Keywords

26S Proteosome, CDC48, SP1, TOC, TOM, Ubiquitination

INTRODUCTION

The plant organelles chloroplasts and mitochondria are derived from two ancient endosymbiotic events, whereby a photosynthetic cyanobacterium and an aerobic prokaryote were separately engulfed by a eukaryotic cell. Over the intervening billion years of evolution, most genes from the endosymbiont genomes have been transferred to the host nucleus. Hence, most chloroplasts and mitochondrial proteins are encoded in the nucleus, synthesized in the cytosol, and imported into the organelles through the TOC (translocon at the outer membranes of chloroplasts) and the TOM (translocon at the outer membranes of mitochondria) complexes, respectively (Duncan et al. 2013; Shi and Theg 2013; Nakai 2018). Components of the TOC complex, including Toc33 and Toc159, are directed to the 26S proteasome by the ubiquitin-dependent chloroplast-associated protein degradation (CHLORAD) system (Ling et al. 2012; Ling et al. 2019). These TOC proteins are first ubiquitinated by SUPPRESSOR OF PPI1 LOCUS1 (SP1), an E3 RING ubiquitin ligase embedded in the chloroplast outer membrane (OM) (Ling et al. 2012). SP1 forms a complex with SP2, an Omp85-type β-barrel channel embedded in the OM, and CDC48A, a cytosolic AAA^+ protein, at the chloroplast surface (Ling et al. 2019). Both SP2 and CDC48A are essential for the re-translocation of TOC components from the OM to the cytosol. SP2 is believed to play a conductance role, while CDC48A pulls the TOC proteins out of the membrane via ATP hydrolysis, after which ubiquitinated TOC proteins are targeted to the 26S proteasome for degradation (Ling et al. 2019). Yet, how ubiquitinated TOC proteins and the SP1/SP2/CDC48A complex are targeted to the 26S proteasome has been unclear. The CHLORAD system is critically important for chloroplast biogenesis, plant development, and stress responses (Ling et al. 2012; Ling and Jarvis 2015; Ling et al. 2019). Overexpression of *SP1* reduces the abundance of TOC complexes (Ling et al. 2012) and confers transgenic plants with higher resistance to salt, osmotic, and reactive oxygen species (ROS) stresses (Ling and Jarvis 2015). A reduction in the import of photosynthesis-related proteins can decrease the amount of ROS generated from chloroplasts during photosynthesis. Although SP1 is also present in mitochondria, whether it is involved in the ubiquitination of the TOM complex is unknown (Pan and Hu 2018). In addition, while the mitochondria-associated protein degradation (MAD) pathways of mitochondrial outer membrane (MOM) proteins are well characterized in yeast and mammalian cells (Zhang and Ye 2016; Zheng et al. 2019), the equivalent plant pathway(s) remain obscure. Here, we discovered a novel plant protein, which participates in ubiquitin-proteasome pathways for the degradation of *Arabidopsis thaliana* TOC and TOM tail-anchored receptors.

RESULTS

A novel cytosolic protein interacts with the C-terminal transmembrane domains of tail-anchored TOC and TOM receptors

We previously showed that Arabidopsis PURPLE ACID PHOSPHATASE2 (PAP2) plays a role in protein import into chloroplasts and mitochondria (Sun et al. 2012; Law

et al. 2015; Zhang et al. 2016; Voon et al. 2021). Similar to Toc33 and Toc34 and to Tom20-2, Tom20-3, and Tom20-4, PAP2 is a tail-anchored (TA) protein anchored on the outer membranes of these two organelles via its hydrophobic C-terminal motif (Sun et al. 2012). PAP2 interacts with the precursor of the small subunit of Rubisco (pSSU) (Zhang et al. 2016) as well as the presequences of several MULTIPLE ORGANELLAR RNA EDITING FACTOR (pMORF) proteins (Law et al. 2015) and plays a role in their import into chloroplasts (Zhang et al. 2016) and mitochondria (Law et al. 2015), respectively. To further elucidate these processes, we first performed a yeast two-hybrid (Y2H) screen to identify PAP2-interacting proteins (Voon et al. 2021). One novel protein encoded by the gene At5g42220 drew our attention, as multiple clones were isolated during screening. The C-terminal transmembrane domain (TMD) of PAP2 was required for its interaction with At5g42220.1 (Fig. 1A). We named the protein encoded by At5g42220.1 TMD-binding protein for tail-anchored outer membrane proteins (TTOP). TTOP is an 879-amino-acid (aa) protein containing a ubiquitin-like (Ubl) domain at its N terminus (aa 24–95), while the rest of the protein lacks known conserved domains.

Y2H analysis of the interaction of TTOP with other tail-anchored (TA) proteins on the outer membranes of chloroplasts and mitochondria revealed an interaction with Tom20-2, Tom20-3, and Tom20-4 (hereafter referred to together as Tom20-2/3/4) (Fig. 1A). The TMDs of the mitochondrial proteins were essential for their interactions with TTOP, as we observed no interaction between TTOP and TMD-truncated versions of Tom20-2/3/4 (Fig. 1A). We did not detect any interaction of TTOP with Toc33 and Toc34 (hereafter Toc33/34) by Y2H (Fig. S1), possibly because the BD-Toc33/34 fusion proteins could not enter the yeast nucleus, as the TA motifs from Toc33/34 and Tom20-2/3/4 have different properties (Sun et al. 2012). We then turned to bimolecular fluorescence complementation (BiFC) to confirm these interactions: TTOP fused to the C-terminal half of yellow fluorescent protein (cY) interacted with fusion proteins between the N-terminal half of YFP (nY) and Toc33/34, Tom20-2/3/4 and PAP2 (Fig. 1B), as determined by the reconstitution of YFP fluorescence. These interactions were dependent on their TMDs (Fig. S2), as there was no interaction between TTOP and TMD-truncated TA proteins (Fig. S3A). Notably, we did not detect interaction between the above TA proteins and TTOP fused to cY at its C terminus (Fig. S3B), indicating that a free TTOP C terminus is essential for these interactions. For TTOP interactions with Tom20-2/3/4, we occasionally observed YFP fluorescence surrounding mitochondria (Fig. 1B), which then appeared in the cytosol after a short duration (Fig. S4). These indicated that TTOP first interacted with Tom20-2/3/4 on the outer membrane of mitochondria and the interacting partners then migrated to the cytosol. For Toc33/34 and PAP2, we did not observe BiFC signals on the organellar outer membranes, but only in the cytosol (Fig. 1B). This observation was not due to a failure of targeting to the outer membranes, as GFP-TA fusions between the green fluorescent protein (GFP) and the TA proteins were successfully targeted to the organellar outer membrane (Fig. S5). These results suggested that TTOP interacts with cytosolic TA proteins carrying free TMDs but not with TA proteins whose TMDs are embedded in

the outer membranes. In agreement with the BiFC results, co-immunoprecipitation (co-IP) assays from protein extracts of transiently co-transfected protoplasts confirmed the physical associations between TTOP and the above TA proteins (Fig. 1C).

TTOP is essential for chloroplast biogenesis

To characterize the role of TTOP in organelle biogenesis and plant development, we first obtained two *ttop* mutants, SALK_128909 and SALK_151742, but these lines did not harbor a T-DNA insertion in *TTOP*, as determined by genotyping PCR. We therefore generated our own *TTOP* knock-out mutants using a highly efficient CRISPR/Cas9 system (Tsutsui and Higashiyama 2017), leading to the isolation of the *ttop-1* and *ttop-5* mutant alleles, with a single-base insertion of an A or T in the 43 bp of the first *TTOP* exon, respectively (Fig. S6A). Both alleles were predicted to introduce a premature stop codon 78 bp into the first exon. We selected Cas9-free *ttop-1* and *ttop-5* mutant lines and confirmed the absence of TTOP accumulation by immunoblotting with anti-TTOP antibodies (Fig. S6B). Both *ttop-1* and *ttop-5* mutants grew normally under standard growth conditions (Fig. S6C). We then attempted to generate transgenic lines overexpressing a construct encoding N-terminal GFP-tagged TTOP (GFP-TTOP), as adding a tag to the C terminus of TTOP affected its interaction with TA proteins in the BiFC assay. However, we failed to obtain lines that overexpressed *GFP-TTOP* when driven by either *UBIQUITIN10* (*UBQ10*) or the cauliflower mosaic virus *35S* promoter, suggesting that constitutive expression of *TTOP* might lead to lethality. Accordingly, we generated stable Arabidopsis transgenic lines expressing *GFP-TTOP* under the control of a dexamethasone (DEX)-inducible promoter (pTA7002-*GFP-TTOP*) (Aoyama and Chua 1997). These pTA7002-*GFP-TTOP* lines grew normally when sown on unadulterated MS medium but not on MS medium containing 10 μM DEX (Fig. 2A, B), confirming that constitutive overexpression of *GFP-TTOP* is early seedling-lethal, possibly due to an influence on chloroplast biogenesis, as indicated by the impairment of chloroplast development in cotyledons (Fig. 2C, D). When 5-day-old pTA7002-*GFP-TTOP* seedlings germinated on MS medium were transferred to MS medium containing 10 μM DEX for 3 days, their cotyledons turned yellow (Fig. 3A) and their chloroplasts degenerated, as evidenced by a decline in chloroplast and thylakoid size (Fig. 3B) observed during transmission electron microscopy (TEM) analysis. We confirmed the high accumulation of GFP-TTOP in pTA7002-*GFP-TTOP* lines by immunoblotting with anti-TTOP antibodies (Fig. 3B). Immunoblotting showed that higher TTOP protein accumulation reduced the abundance of outer envelope proteins in chloroplasts, without affecting the level of Tic40 (Fig. 3C). We failed to analyze mitochondrial proteins by immunoblotting, possible due to the low abundance of mitochondrial proteins in total protein extract and the lack of highly sensitive antibodies. We also tested the response of etiolated *ttop* seedlings to illumination, which induces chlorophyll biosynthesis and cotyledon opening in the wild type: Both *ttop* mutants also showed defects in cotyledon development and lower survival rates (Fig. 3D), as a consequence of impaired chloroplast biogenesis (Fig. 3E), upon exposure to light.

168 **TTOP is expressed in actively dividing tissues**

169 To examine the expression pattern of *TTOP*, we generated transgenic lines
170 harboring a transgene driving the expression of the *β-GLUCURONIDASE* (*GUS*)
171 reporter gene under the control of the *TTOP* promoter (*pTTOP*:*GUS*) (Fig. 4A-I). GUS
172 staining was strong in root and shoot meristems (Fig. 4A–D), which are characterized
173 by actively dividing cells with high energy demand. The *TTOP* promoter was active in
174 young leaves but not in mature leaves (Fig. 4E) and was also active in trichomes,
175 flowers, and pollen (Fig. 4F–I). To determine the cellular localization of TTOP, we
176 generated *ttop-5 pTTOP*:*GFP-TTOP* transgenic plants by transforming the construct
177 *pTTOP*:*GFP-TTOP*, driving *TTOP* expression from the *TTOP* promoter, into *ttop-5*
178 plants. The transgene complemented the *ttop-5* mutant, as evidenced by the rescue of
179 the cotyledon phenotypes (Fig. 3D) upon de-etiolation. These results hinted that *TTOP*
180 expression is strictly controlled. Confocal laser scanning microscopy (CLSM) analysis
181 of stable Arabidopsis *ttop-5 pTTOP*:*GFP-TTOP* seedlings showed that GFP-TTOP
182 accumulated in the cytosol of all tissues tested, including mesophyll cells, the epidermis,
183 the hypocotyl, and the roots, and was highly abundant in the root and shoot meristems
184 and the first true leaves of 6-day-old seedlings (Fig. 4J). The cytosolic location of TTOP
185 is also confirmed in protoplasts (Fig. S5).

186 **TTOP participates in the CHLORAD pathway**

187 As TTOP interacted with TA proteins targeted to chloroplasts and mitochondria,
188 we generated *p35S:mCherry-Toc33* and *p35S:mCherry-Tom20-2* transgenic plants in
189 the *ttop-5* mutant background. We then crossed these transgenic lines with wild-type
190 (WT) plants and selected homozygous *p35S:mCherry-Toc33* and *p35S:mCherry-*
191 *Tom20-2* transgenic plants in the WT background from their progeny. With this crossing
192 strategy, we thus obtained *p35S:mCherry-Toc33* and *p35S:mCherry-Tom20-2*
193 transgenic plants in the WT and *ttop-5* backgrounds carrying the same T-DNA insertion
194 events, allowing us to compare mCherry-Toc33 and mCherry-Tom20-2 protein
195 abundance. The abundance of mCherry-Toc33 and mCherry-Tom20-2 was the same in
196 the two WT lines (Fig. 4K). Importantly, mCherry-Toc33 and mCherry-Tom20-2
197 abundance was much higher in *ttop-5* relative to the WT lines, as evidenced by
198 immunoblotting with anti-mCherry antibodies (Fig. 4K). We thus concluded that TTOP
199 may contribute to the degradation of Toc33 and Tom20-2, which prompted us to explore
200 whether TTOP participates in the CHLORAD pathway. BiFC analysis showed that
201 TTOP interacts with SP1, CDC48A, and the 26S proteasome subunits REGULATORY
202 PARTICLE NON-ATPASE6 (RPN6), RPN10, RPN12, and RPN13a (Fig. 5A), but not
203 with SP2. In agreement with this, co-IP assays from transiently transfected protoplast
204 extracts showed that TTOP can pull down SP1, CDC48, RPN6, RPN10, RPN12 and
205 RPN13 (Fig. 5B). Co-transfection of *mCherry-TTOP*, *cY-CDC48A*, and *nY-*
206 *Toc33/Toc34* constructs in Arabidopsis protoplasts resulted in the reconstitution of YFP
207 fluorescence and co-localization of YFP with mCherry fluorescence in the cytosol,
208 indicating that these proteins co-localize (Fig. 6). Likewise, co-transfection of *cY-*
209 *CDC48A*, and *nY-Tom20-2/Tom20-3/Tom20-4* constructs in protoplasts also
210 demonstrated their co-localization in the cytosol and exhibited a network appearance

211 (Fig. 7), which disappeared when TTOP was co-expressed (Fig. 6). CDC48A interacted
212 with Toc33/34 and Tom20-2/3/4 at the periphery of chloroplasts and mitochondria, as
213 indicated by BiFC assays (Fig. 7). We repeated the BiFC assays in protoplasts prepared
214 from *ttop-5* plants and observed the same results (Fig. S7), indicating that TTOP is not
215 essential for the interaction of CDC48A with Toc33/34 or Tom20-2/3/4.
216
217 **TTOP may participate in a ubiquitin-dependent MAD pathway**
218 Next, we tested whether SP1 can ubiquitinate Toc33 and Tom20-3 by *in vitro*
219 ubiquitination assays. Recombinant Arabidopsis UBIQUITIN-ACTIVATING
220 ENZYME1 (UBA1), UBIQUITIN CONJUGATING ENZYME8 (UBC8), and
221 ubiquitin (Fig. S8), recombinant SP1flex, TTOP (Fig. S9) and Toc33 and Tom20-3 (Fig.
222 S10) were purified in *E. coli*. GST-SP1RING, but not SP1flex, self-ubiquitinated (Fig.
223 S11A). These data showed that the SP1RING domain is able to ubiquitinate its GST
224 fusion partner, whereas SP1flex which contains SP1RING domain cannot self-
225 ubiquitinated itself. SP1flex also ubiquitinated full length Toc 33 (Toc33FL, a.a. 1-297)
226 and Toc33 without the C-terminus (Toc33NC, a.a. 1-251) (Fig. S11B). GST-TTOP, but
227 not GST alone, pulled down both non-ubiquitinated (Fig. S11C) and ubiquitinated
228 Toc33FL (Fig. S11D), but not Toc33NC in either form (Fig. S11E), indicating that SP1
229 ubiquitinates the receptor domain of Toc33, whereas TTOP binds to the TMD motif of
230 Toc33, independent of its ubiquitination status. SP1flex/UBC8 did not ubiquitinate
231 Tom20-3 without the C-terminus (Tom20-3NC, a.a. 1-174) or TTOP (Fig. S11F).
232 Unidentified E2/E3 ligase(s) in seedling extracts appeared to ubiquitinate His-Tom20-
233 3NC, which was not pulled down by GST-TTOP due to the lack of the TMD motif of
234 Tom20-3 (Fig. S11G). Although we could not test the ubiquitination of full length
235 Tom20-3 as we failed to express it in *E. coli*, the TMD motifs of Tom20-2/3/4 cannot
236 be ubiquitinated as they do not contain any lysine residues. Therefore, the ubiquination
237 sites must be located at the cytosolic domain of Tom20-3. Unknown E3 ligase(s) in the
238 plant extracts may therefore ubiquitinate Tom20-3, or SP1 at the mitochondrial OM
239 (Pan and Hu 2018) may still act as the cognate E3 ligase of Tom20-3, as our *in vitro*
240 experiments did not test all 37 Arabidopsis E2 ligases. Further studies are required to
241 delineate the details of the ubiquitin-dependent MAD pathway.

242 **TTOP binds to RPN13 of the 26S Proteosome via its N-terminal UBL domain.**
243 Using the TTOP protein sequence to PBLAST the proteins in the human genome,
244 the protein with the highest protein sequence identity was human BAG6 (Chio et al.
245 2017; Shao et al. 2017). The length of BAG6 (1132 a.a.) is much longer than TTOP
246 (879 a.a.) and they only share 23% protein sequence identity, mainly at their N-terminal
247 UBL domains and their C-terminal BAG domain (Mock et al. 2015). In mammalian
248 system, the Bag6/Ubl4A/Trc35 complex directs mislocated polypeptides on the ER
249 membrane toward 26S proteasome for degradation to avoid protein aggregations in the
250 cytosol (Hessa et al. 2011; Wang et al. 2011). Besides BAG6, many UBL-containing
251 proteins are involved in shuttling ubiquitinated substrates to 26S proteasomes and some
252 UBL domains were shown to bind to RPN subunits (Chen et al. 2016; Shi et al. 2016).
253 Here, we employed AlphaFold2 (Jumper et al. 2021; Mirdita et al. 2021) to predict the

interaction between the UBL domain of TTOP with the RPN proteins we identified by BiFC. As predicted by AlphaFold2, the UBL domain of TTOP could interact with the pleckstrin-like receptor for ubiquitin (PRU) domain of RPN13 (Fig. S12D and Fig. 8A). The interaction between these two domains was confirmed by ITC experiment and the affinity was determined to be 29 μM (Fig. 8D). In addition, sequence alignment with the UBL domain of BAG6 showed that TTOP UBL contains the RNF126_NZF interacting residues (Krysztofinska et al. 2016), suggesting that TTOP UBL may have a zinc finger (ZF) binding ability (Fig. S13A). SP1 RING is a ZF protein with the E3 ligase function (Pan and Hu 2018; Ling et al. 2019) and Alphafold2 predicted that the UBL domain of TTOP could bind to SP1 RING, too (Fig. S13B). By contrast, the C-terminus of TTOP contains a BAG domain that contains conserved Ubl4A interaction residues (Mock et al. 2015) and this domain was predicted to be able to bind human Ubl4A by AlphaFold2 (Fig. S14).

Heat treatment induces TTOP-dependent clearance of mCherry-Toc and mCherry-Tom20-2 in planta

We noticed that heat treatment can induce patch formation of GFP-TTOP in protoplasts (Fig. S15A). Then we generated double expression lines by transforming the homozygous DEX-GFP-TTOP line with the *p35S:mCherry-Toc33* and *p35S:mCherry-Tom20-2* constructs to carry out heat-induction experiment. These lines expressed mCherry-Toc33 and mCherry-Tom20-2 constitutively at high levels. GFP-TTOP was induced by 24h Dex treatment in some 8-day-old seedlings and then subject to 30 min heat treatment at 45°C. While the mCherry signals could still be seen immediately after the heat treatment, the signals of mCherry-Toc33 and mCherry-Tom20-2 gradually disappeared (1h and 3h post treatment) when GFP-TTOP was present, but remained when GFP-TTOP was absence (Fig. 9 and Fig. S16). These in planta data showed that GFP-TTOP is required for the degradation of mCherry-Toc33 and mCherry-Tom20-2. Heat treatment was also shown to induce mRNA expression of TTOP (Fig. S15B) and the *ttop-5* mutants were less heat-resistant than the WT seedlings (Fig. S15C).

DISCUSSION

In this study, we discovered a converged pathway for the delivery of ubiquitinated tail-anchored receptors of the TOC and TOM complexes to the 26S proteasome for degradation (Fig. 10). In CHLORAD, a system for the clearance of the TOC complex by the ubiquitin-proteasome system, the E3 ligase SP1 mediates the ubiquitination of the TOC complex, while SP2 and the AAA^+ ATPase CDC48A act as a conduit and a motor, respectively, to retrotranslocate the ubiquitinated TOC complex and SP1 out of the chloroplast OM (Ling et al. 2019). However, how the retrotranslocated, ubiquitinated TOC proteins are delivered to the 26S proteasome was not clear. Here, we showed that TTOP is the cytosolic shuttling factor responsible for the delivery of the ubiquitinated TOC proteins to the 26S proteasome. Our observations fit with the previous findings that CDC48 plays a role in the retrotranslocation of ubiquitinated

297 Toc33 and SP1 from chloroplasts to cytosol (Ling et al. 2019). TTOP interacts with
298 TOC proteins and SP1 in the cytosol after they are retrotranslocated from the
299 chloroplast OM by CDC48. In addition, our data suggested the existence of a similar
300 MAD pathway for the removal of Tom20 from the mitochondrial OM, which involves
301 uncharacterized E2/E3 ligases, CDC48A, and TTOP. In this pathway, ubiquitinated
302 Tom20 receptors of the TOM complexes are retrotranslocated from the OM to the
303 cytosol, followed by the delivery of the complex to the 26S proteasome by TTOP.
304 Ubiquitination of the TOC and TOM receptors is not required for TTOP binding; hence,
305 the binding takes place after these receptors are retrotranslocated from the OMs to the
306 cytosol. During TOC biogenesis, cytosolic Arabidopsis ankyrin repeat protein 2A
307 (AKR2A) binds to the TMDs of newly synthesized Toc33 and Toc34, but not that of
308 Tom20-2, when they are released from ribosomes to maintain the nascent TOC
309 receptors from forming aggregates or binding to non-specific hydrophobic proteins
310 before their insertion into the chloroplast OM (Bae et al. 2008; Kim et al. 2019). Our
311 BiFC data showed that TTOP first interacted with Tom20-2/3/4 on the OM of
312 mitochondria (Fig. 1B), and the complexes migrated to cytosol after a short duration
313 (Fig. S4). Future research is required to identify the E2/E3 ligases that ubiquitinate
314 Tom20 receptors and the role of CDC48 in their retrotranslocation. For Toc33/34, we
315 did not observe BiFC signals on the chloroplast outer membranes, but only in the
316 cytosol (Fig. 1B). Perhaps the retrotranslocation of Toc33/34 happened more efficiently
317 than that of Tom20-2/3/4 in the BiFC experiments. Nonetheless, while both AKR2A
318 and TTOP can bind to the TMDs of Toc33 and Toc34, they might bind to the receptors
319 at different processes: the biogenesis and degradation stages of the TOC complexes,
320 respectively.

321 Besides the UBL domain at its N-terminus and the BAG domain at its C-terminus,
322 the other region of TTOP does not show any sequence homology to any known
323 structures. In the mammalian Bag6/Ubl4A/Trc35 complex, the C-terminal BAG
324 domain of BAG6 interacts with UblA4 (Mock et al. 2015), which in turn interacts with
325 the small glutamine-rich tetratricopeptide repeat-containing protein alpha (SGTA), and
326 the latter binds TMD directly (Shao et al. 2017; Guna and Hegde 2018). Different from
327 the BAG6 in the mammalian system, TTOP can bind to TMDs of the TOC/TOM TA
328 receptors directly. Although the BAG domain at the C-terminus of TTOP was predicted
329 to be able to interact with human UblA4 by Alphafold2 (Fig. S14), PBLAST search
330 could not find any homolog of UblA4 in Arabidopsis and the closet homolog of SGTA
331 are proteins containing the tetratricopeptide repeat (TPR) domains, including
332 HOP1(Fellerer et al. 2011), HOP2, HOP3 (Fernández-Bautista et al. 2017), OM64
333 (Panigrahi et al. 2014) and Toc64 (Sommer et al. 2013), of which they only share
334 homology with SGTA at their TPR domains. It might be interesting to investigate
335 whether these proteins could bind to TMDs and play a role similar to SGTA in the plant
336 system.

337 Although BiFC data showed that TTOP interacted with RPN6/10/12/13,
338 Alphafold2 only predicted that the UBL domain of TTOP could interact with the pru

339 domain of RPN13 (Fig. 8A). This interaction was experimentally confirmed by ITC
340 experiment (Fig. 8D). The interaction affinity (29 μM) is comparable to the affinity
341 between human RPN13^{PRU} domain with the UBL domain of hPLC2 (9.5 μM) (Chen et
342 al. 2016; VanderLinden et al. 2017) and the affinity between human RPN13^{PRU} domain
343 with the UBL domain of human HR23a (26 μM) (Husnjak et al. 2008; Chen et al. 2016),
344 and is stronger than the affinity between human RPN13^{PRU} domain with ubiquitin (91
345 μM) (VanderLinden et al. 2017). This mean that TTOP could have the similar 26S
346 interaction ability like that of hPLC2 and HR23a. Bear in mind that the a.a. sequence
347 between residues 96 – 826 of TTOP is completely novel and no structure can be
348 predicted, it is not known if this region of TTOP could interact with the other RPN
349 subunits. While Alphafold2 may not be able to predict all interactions precisely, it is
350 also possible that not all BiFC signals were generated from direct interaction between
351 TTOP and these RPN subunits (Fig. 5). It is also possible that the binding of TTOP and
352 RPN13 may indirectly enhance the formation of complex between TTOP and the other
353 RPN subunits. The interaction between TTOP and 26S proteosome could become
354 stronger when more than one interacting partner is involved. Without binding to
355 ubiquitinated substrates, 26S proteosome is inactive (Eisele et al. 2018). All seven
356 tested UBL-containing proteins were able to stimulate peptide hydrolysis of 26S
357 proteosome, and all three tested UBL-containing proteins were able to stimulate ATPase
358 activities of 26S proteosome (Collins and Goldberg 2020). It will be interesting to
359 investigate whether plant UBL-containing proteins, such as TTOP, could also activate
360 plant 26S proteosomes.

361 The E1/E2/E3 ligase-CDC48A-TTOP-26S proteasome degradation pathway may
362 also apply to the plant Tom20 receptors. In yeast, a ubiquitin-proteasome pathway for
363 the degradation of Tom70, a TOM receptor lacking a plant ortholog (Ghifari et al. 2018),
364 has been characterized (Wu et al. 2016). Tom70 is ubiquitinated by the cytosolic E3
365 ligase RSP5 (Reverses Spt-Phenotype 5) and binds to the ubiquitin binding domain of
366 Doa1 (Degradation Of Alpha 1), which in turn binds to Cdc48 of the Cdc48/Ufd1/Npl4
367 complex via its C-terminal PUL domain (Mullally et al. 2006). Surprisingly, this
368 ubiquitin-proteasome pathway is specific to Tom70, as it does not target the other yeast
369 TOM receptor, Tom22, for degradation (Wu et al. 2016). In addition to this pathway for
370 mitochondrial OM proteins, yeast also possesses a mitochondrial protein translocation-
371 associated degradation (mitoTAD) pathway. The transmembrane protein Ubx2
372 (Ubiquitin regulatory X 2), which associates with the TOM complexes, can recruit the
373 Cdc48/Ufd1/Npl4 complex (Schuberth and Buchberger 2005) to remove clogged
374 precursor proteins from the TOM channel (Martensson et al. 2019). Our results revealed
375 that there is a converged ubiquitin-proteasome degradation pathway, mediated by
376 specific E3 ligases, CDC48 and TTOP, for tail-anchored receptors of TOC and TOM in
377 Arabidopsis. This pathway is important for chloroplast (Ling et al. 2012) and
378 chromoplast biogenesis (Ling et al. 2021), etiolation (Fig. 3D) and heat stress (Fig. S15).
379 It is unclear how depletion of the components of the CHLORAD pathways, such as SP1
380 (Ling et al. 2012) and TTOP (Fig. 3E), affect chloroplast biogenesis. Depletion of the
381 CHLORAD pathways may cause accumulation of the receptor components of the TOC

complexes (Fig. 4K), which may affect the stoichiometry and thus the assembly of the TOC complexes. The accumulation of the TOC receptors may enhance ROS production under stresses. The CHLORAD pathway has been shown to help plants to respond to salinity and osmotic stresses by depleting TOC complexes and thus reducing ROS production from the photosystems (Ling and Jarvis 2015). Here, we showed that heat stress can induce TTOP mRNA transcription and *ttop* mutants are more sensitive to heat stress (Fig. S15). Hence, the CHLORAD pathway may also respond to heat stress and could alleviate heat stress by depleting TOC complexes and reducing heat-induced ROS. *TTOP* is also highly expressed in active sites of cell division (Fig. 4A-J), where mitochondria are abundant and active to meet the high energy demand of cell division. Nonetheless, loss of *TTOP* function did not affect plant growth under normal growth conditions. Perhaps TTOP is required only when the turnover of TOC and TOM receptors is extremely high (e.g., during etiolation) and under stresses (e.g. heat). When their turnover is low, the absence of TTOP may not cause significant phenotypes, possibly because of a lower chance of protein aggregation of TOC and TOM receptors. There is only one *TTOP* gene in the Arabidopsis genome, and no homologous protein has been identified in any non-plant species (Fig. S17). Hence, this converged ubiquitin-proteasome pathway for the degradation of tail-anchored receptors may have co-evolved with the TOC/TOM receptors during the endosymbiosis processes in plant species. While the general steps (ubiquitination by E3 ligases, retrotranslocation by CDC48, shuttling to 26S proteosomes by UBL-containing proteins, and 26S proteosome degradation) are in common, there are mechanistic differences between the animal and plant systems. In term of masking the TMD motifs of TA receptors to prevent protein aggregation during their cytosolic shuttling to 26S proteosome, plant TTOP can bind to TMDs directly, whereas animal BAG6 requires bridging to SGTA via Ubl4A for TMD binding. TTOP may evolve for direct binding to the TMDs of both TOC/TOM TA receptors to simplify the process.

MATERIALS AND METHODS

Plant growth conditions and generation of mutants and transgenic lines

All wild-type, mutant, and transgenic Arabidopsis (*Arabidopsis thaliana*) plants used in this study were from the Columbia-0 accession (Col-0). Plants were grown on soil or on Murashige-Skoog (MS) agar medium in petri plates at 22°C under a 16-h-light/8-h-dark cycle using cool white fluorescent light bulbs (100 μmol m^{-2} s^{-1}). Seeds were surface sterilized, sown on half-strength MS medium with 1% (w/v) sucrose (pH 5.8-6.2), stratified at 4°C in the dark for 3 days, and then released in a growth chamber.

To generate transgenic plants, all constructs were introduced into Agrobacterium (*Agrobacterium tumefaciens* GV3101 strain) and transformed into plants by the floral dip method (Clough and Bent 1998). The transgenic plants were selected based on resistance to the appropriate antibiotic, and then protein accumulation in the plants was confirmed by confocal microscopy or immunoblotting. Homozygous lines were obtained after propagation and selection for several generations and used for experiments. To induce the expression of *TTOP* in pTA7002-*GFP-TTOP* plants, 10 μM

425 DEX (10 mM stock dissolved in DMSO) was added to the culture medium or 25 μM
426 DEX was dissolved in ddH_2O and sprayed on the plants. The equivalent volume of
427 DMSO was added to the culture medium or ddH_2O as negative control. The *ttop* knock-
428 out mutants were generated using a CRISPR/Cas9 system (Pan et al. 2016). The
429 designed single guide RNA (sgRNA) sequence CTCTAGTAGCACCAATGCGT was
430 cloned into plasmid pKI1.0R and the plasmid transformed into Col-0 (WT) plants. The
431 transformants were selected by antibiotic resistance. The *ttop* mutants were identified
432 from the above selected transformants by genomic PCR and sequencing. To ensure
433 genetic stability, Cas9-free *ttop* mutants that did not carry the CRISPR/Cas9 cassette
434 were obtained by selecting only those seeds showing no red fluorescence under a
435 stereomicroscope (model SZX16, Olympus). The Cas9-free seedlings were grown to
436 maturity and their progeny used for experiments.
437 The *ttop-5 p35S:mCherry-Toc33* transgenic plants were generated by
438 transforming the plasmid *p35S::mCherry-Toc33* into the *ttop-5* mutant. Homozygous
439 *ttop-5 p35S:mCherry-Toc33* plants were obtained and crossed to WT plants, and WT
440 transgenic plants harboring the *p35S:mCherry-Toc33* transgene were selected from the
441 second generation of the crossed plants by sequencing of the respective PCR-amplified
442 genomic sequences. Two individual homozygous transgenic lines expressing mCherry-
443 Toc33 in the *ttop-5* and WT backgrounds were obtained: *ttop-5 p35S:mCherry-Toc33*
444 #1, *ttop-5 p35S:mCherry-Toc33* #2, *p35S:mCherry-Toc33* #1, and *p35S:mCherry-*
445 *Toc33* #2. Similarly, *ttop-5 p35S:mCherry-Tom20-2* transgenic plants were generated
446 by transforming the construct *p35S:mCherry-Tom20-2* into the *ttop-5* mutant
447 background. Homozygous *ttop-5 p35S:mCherry-Tom20-2* plants were then crossed to
448 WT plants, and WT plants harboring the *p35S::mCherry-Tom20-2* transgene were
449 identified. Two individual transgenic lines each in the *ttop-5* and WT background were
450 obtained: *ttop-5 p35S:mCherry-Tom20-2* #1 and *ttop-5 p35S:mCherry-Tom20-2* #2,
451 and *p35S:mCherry-Tom20-2* #1 and *p35S:mCherry-Tom20-2* #2.
452 De-etiolation experiments were performed as reported previously (Ling et al.
453 2012). Seeds harvested from the same growth batch were sown on MS medium,
454 stratified at 4°C in the dark for 3 days, and then exposed to light for 6 h to induce
455 germination. Next, the seedlings were grown in the dark for 6 days and transferred to
456 continuous light for different periods, and their survival rates and seedling growth
457 phenotypes were recorded. Organellar morphology in cotyledons was examined by
458 transmission electron microscopy (TEM). Each experiment was performed
459 independently four times, and more than 100 seedlings per genotype were used in each
460 experiment for survival rate analysis.
461 To mark mitochondria in plant cells, seedlings were incubated in half-strength MS
462 liquid culture medium containing 1 mM MitoTracker (Thermo Fisher Scientific, USA)
463 for 30 min, and the dye was removed by washing with culture medium twice. To induce
464 the expression of *TTOP* in pTA7002-*GFP-TTOP* transgenic plants, seedlings were
465 grown on MS medium containing 10 μM dexamethasone (DEX) or sprayed with 25
466 μM DEX dissolved in ddH_2O.
467
468 **Yeast two-hybrid, protoplast transient expression, and BiFC assays**

Yeast two-hybrid analysis was performed using the MatchMaker GAL4 Two-Hybrid System 3 (Clontech, USA) according to the manufacturer's instructions. The different CDSs were cloned into the pGBKT7 or pGADT7 vector. Pairs of pGBKT7 and pGADT7 vectors carrying the appropriate CDSs were co-transformed into the Y2HGold yeast strain. Diploids were selected on synthetic defined (SD) medium lacking tryptophan (Trp) and leucine (Leu) (SD –Trp –Leu) to select transformants. The colonies growing on SD –Trp –Leu medium were then transferred to selective SD medium lacking histidine (His), Trp, and Leu (SD –His –Trp –Leu) or lacking adenine (Ade), His, Trp, and Leu (SD –His –Ade –Trp –Leu) and were incubated at 30°C for 3–6 days to investigate protein–protein interactions. The control vector pairs pGADT7-T and pGBKT7-lam, and pGADT7-T and pGBKT7-53 were co-transformed into yeast as negative and positive controls, respectively. Yeast colonies were grown on selective SD –His –Ade –Trp –Leu medium. The experiments were repeated three times independently with similar results.

Arabidopsis mesophyll protoplast preparation and transfection were performed according to a previously described method (Yoo et al. 2007). Protoplasts were isolated from rosettes of 4-week-old Col-0 plants grown on soil by incubating the rosettes with enzyme solution containing 1% (w/v) cellulose (Onozuk R-10, Yakult, Japan) and 0.2% (w/v) macerozyme (R-10, Yakult, Japan) for 2–4 h. The isolated protoplasts were washed with W5 buffer three times to thoroughly remove the enzymes. PEG4000 was used to transfect plasmids into protoplasts; 0.1 mL (10^5) of protoplasts was transfected with 8 μg of DNA. The transfected protoplasts were cultured for 12 h in darkness to allow protein accumulation and were collected for fluorescence detection or protein extraction. To mark the mitochondria in the cells, protoplasts were incubated in W5 culture medium containing 100 nM MitoTracker for 20 min, and excess MitoTracker was removed by washing with W5 culture medium twice. For heat treatment, the protoplasts were incubated at 37 °C for 30 min before confocal observation.

For the BiFC assay, Arabidopsis mesophyll protoplasts were co-transfected with the appropriate pairs of constructs carrying either *nY* or *cY*, fused to different CDSs, and cultured overnight (12 h) for protein expression. The reconstitution of YFP fluorescence, indicating protein–protein interaction, was detected by fluorescence microscopy using a confocal microscope. For each experiment, more than 40 individual cells were analyzed by confocal imaging that represented >90% of cells that showed similar protein expression levels and patterns. Images were captured using a Leica SP8 laser scanning confocal microscope (Leica Microsystems, German). To avoid possible cross-talk between the fluorescence channels, sequential scanning was used when necessary. Images were processed and assembled using Photoshop CS6 software (Adobe, USA).

Statistical analysis

Statistical calculations (mean, SEM, and *t* test) were performed using Microsoft Excel software. The statistical significance of differences between two experimental groups was assessed using a two-tailed Student's *t*-test. Differences between two datasets were considered significant at $P < 0.05$.

513
514 **Accession numbers**
515 The Arabidopsis Genome Initiative locus identifiers for the genes mentioned in this
516 article are as follows: *TTOP* (At5g42220), *Toc33* (At1g02280), *Toc34* (At5g05000),
517 *Tom20-2* (At1g27390), *Tom20-3* (At3g27080), *Tom20-4* (At5g40930), *PAP2*
518 (At1g13900), *CDC48A* (At3g09840), SP1 (At1g63900), *SP2* (At3g44160), *RPN6*
519 (At1g29150), *RPN10* (At4g38630), *RPN12* (At1g64520), *RPN13* (At2g26590),
520 *AtUba1* (At2g30110), *AtUbc8* (At5g41700), and *AtUb* (At4g02890).
521
522 **Data analysis**
523 All data are presented as means with standard errors (mean ± SEM). The collected
524 data were analyzed for statistical significance using analysis of variance (ANOVA)
525 with Tukey's HSD, paired *t*-tests, or unpaired *t*-tests at $P < 0.001$, $P < 0.01$, and $P <$
526 0.05 by SPSS (version 22).
527
528 **Data and materials availability**
529 All data are available in the main text or the supplementary materials. Materials
530 are available from the corresponding authors upon request.
531
532 **ACKNOWLEDGEMENTS**
533 This work was supported by the Science, Technology and Innovation Commission of
534 Shenzhen Municipality (Basic Research Program 201708183000803); the Hong Kong
535 Research Grants Council Area of Excellence Scheme (AoE/M-403/16), and the
536 Innovation and Technology Fund (Funding Support to State Key Laboratory of
537 Agrobiotechnology) of the Hong Kong Special Administrative Region, China. Any
538 opinions, findings, conclusions or recommendations expressed in this publication do
539 not reflect the views of the Government of the Hong Kong Special Administrative
540 Region or the Innovation and Technology Commission.
541
542 **AUTHOR CONTRIBUTIONS**
543 B.L.L. and M.Y. designed the study. S.L.L., J.Y.Z., and K.C.C. generated the majority
544 of constructs and plant transgenic lines. S.C. carried out the *in vitro* ubiquitination
545 experiments and AlphaFold2 prediction. Z.Z. carried out phylogenetic analysis. L.Y.
546 carried out some BiFc experiments. M.Y. generated some constructs and plant lines and
547 carried out all the remaining experiments. B.L.L. and M.Y. wrote the manuscript. All
548 authors revised and approved the manuscript.
549
550 **CONFLICT OF INTEREST.** None declared.
551
552 **REFERENCES**

553 Aoyama T, Chua NH (1997) A glucocorticoid-mediated transcriptional induction system in transgenic
554 plants. **Plant Journal** 11: 605-612
555 Bae W, Lee YJ, Kim DH, Lee J, Kim S, Sohn EJ, Hwang I (2008) AKr2A-mediated import of chloroplast
556 outer membrane proteins is essential for chloroplast biogenesis. **Nat Cell Biol** 10: 220-U101

557 Chen X, Randles L, Shi K, Tarasov Sergey G, Aihara H, Walters Kylie J (2016) Structures of Rpn1
558 T1:Rad23 and hRpn13:hPLIC2 reveal distinct binding mechanisms between substrate receptors and
559 shuttle factors of the proteasome. **Structure** 24: 1257-1270
560 Chio US, Cho H, Shan SO (2017) Mechanisms of tail-anchored membrane protein targeting and
561 insertion. **Annu Rev Cell Dev Biol** 33: 417-438
562 Clough SJ, Bent AF (1998) Floral dip: a simplified method for Agrobacterium-mediated transformation
563 of Arabidopsis thaliana. **The Plant journal : for cell and molecular biology** 16: 735-743
564 Collins GA, Goldberg AL (2020) Proteins containing ubiquitin-like (Ubl) domains not only bind to 26S
565 proteasomes but also induce their activation. **Proceedings of the National Academy of Sciences** 117:
566 4664-4674
567 Duncan O, Murcha MW, Whelan J (2013) Unique components of the plant mitochondrial protein
568 import apparatus. **Biochimica et Biophysica Acta (BBA) - Molecular Cell Research** 1833: 304-313
569 Eisele MR, Reed RG, Rudack T, Schweitzer A, Beck F, Nagy I, Pfeifer G, Plitzko JM, Baumeister W, Tomko
570 RJ, Jr., Sakata E (2018) Expanded coverage of the 26S proteasome conformational landscape reveals
571 mechanisms of peptidase gating. **Cell Rep** 24: 1301-1315.e1305
572 Fellerer C, Schweiger R, Schongruber K, Soll J, Schwenkert S (2011) Cytosolic HSP90 cochaperones HOP
573 and FKBP interact with freshly synthesized chloroplast preproteins of Arabidopsis. **Molecular plant** 4:
574 1133-1145
575 Fernández-Bautista N, Fernández-Calvino L, Muñoz A, Castellano MM (2017) HOP3, a member of the
576 HOP family in Arabidopsis, interacts with BiP and plays a major role in the ER stress response. **Plant,**
577 **cell & environment** 40: 1341-1355
578 Ghifari AS, Gill-Hille M, Murcha MW (2018) Plant mitochondrial protein import: the ins and outs.
579 **Biochem J** 475: 2191-2208
580 Guna A, Hegde RS (2018) Transmembrane domain recognition during membrane Protein biogenesis
581 and quality control. **Current Biology** 28: R498-R511
582 Hessa T, Sharma A, Mariappan M, Eshleman HD, Gutierrez E, Hegde RS (2011) Protein targeting and
583 degradation are coupled for elimination of mislocalized proteins. **Nature** 475: 394-397
584 Husnjak K, Elsasser S, Zhang N, Chen X, Randles L, Shi Y, Hofmann K, Walters KJ, Finley D, Dikic I (2008)
585 Proteasome subunit Rpn13 is a novel ubiquitin receptor. **Nature** 453: 481-488
586 Jumper J, Evans R, Pritzel A, Green T, Figurnov M, Ronneberger O, Tunyasuvunakool K, Bates R, Zidek
587 A, Potapenko A, Bridgland A, Meyer C, Kohl SAA, Ballard AJ, Cowie A, Romera-Paredes B, Nikolov S,
588 Jain R, Adler J, Back T, Petersen S, Reiman D, Clancy E, Zielinski M, Steinegger M, Pacholska M,
589 Berghammer T, Bodenstein S, Silver D, Vinyals O, Senior AW, Kavukcuoglu K, Kohli P, Hassabis D (2021)
590 Highly accurate protein structure prediction with AlphaFold. **Nature** 596: 583-589
591 Kim J, Na YJ, Park SJ, Baek SH, Kim DH (2019) Biogenesis of chloroplast outer envelope membrane
592 proteins. **Plant cell reports** 38: 783-792
593 Krysztofinska EM, Martínez-Lumbreras S, Thapaliya A, Evans NJ, High S, Isaacson RL (2016) Structural
594 and functional insights into the E3 ligase, RNF126. **Sci Rep-Uk** 6: 26433
595 Law YS, Zhang R, Guan X, Cheng S, Sun F, Duncan O, Murcha M, Whelan J, Lim BL (2015)
596 Phosphorylation and dephosphorylation of the presequence of pMORF3 during import into
597 mitochondria from *Arabidopsis thaliana*. **Plant Physiology** 169: 1-12
598 Ling Q, Huang W, Baldwin A, Jarvis P (2012) Chloroplast biogenesis is regulated by direct action of the
599 ubiquitin-proteasome system. **Science (New York, N.Y.)** 338: 655-659
600 Ling Q, Jarvis P (2015) Regulation of Chloroplast Protein Import by the Ubiquitin E3 Ligase SP1 Is

601 Important for Stress Tolerance in Plants. **Curr Biol** 25: 2527-2534
602 Ling Q, Sadali NM, Soufi Z, Zhou Y, Huang B, Zeng Y, Rodriguez-Concepcion M, Jarvis RP (2021) The
603 chloroplast-associated protein degradation pathway controls chromoplast development and fruit
604 ripening in tomato. **Nature Plants** 7: 655-666
605 Ling QH, Broad W, Trosch R, Topel M, Sert TD, Lymperopoulos P, Baldwin A, Jarvis RP (2019) Ubiquitin-
606 dependent chloroplast-associated protein degradation in plants. **Science** 363: aav4467
607 Martensson CU, Priesnitz C, Song J, Ellenrieder L, Doan KN, Boos F, Floerchinger A, Zufall N, Oeljeklaus
608 S, Warscheid B, Becker T (2019) Mitochondrial protein translocation-associated degradation. **Nature**
609 569: 679-683
610 Mirdita M, Ovchinnikov S, Steinegger M (2021) ColabFold - Making protein folding accessible to all.
611 **bioRxiv**: 2021.2008.2015.456425
612 Mock J-Y, Chartron JW, Zaslaver Ma, Xu Y, Ye Y, Clemons WM (2015) Bag6 complex contains a minimal
613 tail-anchor-targeting module and a mock BAG domain. **Proceedings of the National Academy of**
614 **Sciences** 112: 106-111
615 Mullally JE, Chernova T, Wilkinson KD (2006) Doa1 is a Cdc48 adapter that possesses a novel ubiquitin
616 binding domain. **Mol Cell Biol** 26: 822-830
617 Nakai M (2018) New Perspectives on Chloroplast Protein Import. **Plant and Cell Physiology** 59: 1111-
618 1119
619 Pan R, Satkovich J, Hu J (2016) E3 ubiquitin ligase SP1 regulates peroxisome biogenesis in Arabidopsis.
620 **Proc Natl Acad Sci U S A** 113: E7307-E7316
621 Pan RH, Hu JP (2018) The Arabidopsis E3 Ubiquitin Ligase SP1 Targets to Chloroplasts, Peroxisomes,
622 and Mitochondria. **Plant Physiology** 176: 480-482
623 Panigrahi R, Whelan J, Vrielink A (2014) Exploring ligand recognition, selectivity and dynamics of TPR
624 domains of chloroplast Toc64 and mitochondria Om64 from *Arabidopsis thaliana*. **Journal of**
625 **molecular recognition : JMR** 27: 402-414
626 Schuberth C, Buchberger A (2005) Membrane-bound Ubx2 recruits Cdc48 to ubiquitin ligases and their
627 substrates to ensure efficient ER-associated protein degradation. **Nat Cell Biol** 7: 999-1006
628 Shao S, Rodrigo-Brenni MC, Kivlen MH, Hegde RS (2017) Mechanistic basis for a molecular triage
629 reaction. **Science** 355: 298-302
630 Shi L-X, Theg SM (2013) The chloroplast protein import system: From algae to trees. **Biochimica et**
631 **Biophysica Acta (BBA) - Molecular Cell Research** 1833: 314-331
632 Shi Y, Chen X, Elsasser S, Stocks BB, Tian G, Lee B-H, Shi Y, Zhang N, Poot SAHd, Tuebing F, Sun S,
633 Vannoy J, Tarasov SG, Engen JR, Finley D, Walters KJ (2016) Rpn1 provides adjacent receptor sites for
634 substrate binding and deubiquitination by the proteasome. **Science** 351: aad9421
635 Sommer M, Rudolf M, Tillmann B, Tripp J, Sommer MS, Schleiff E (2013) Toc33 and Toc64-III cooperate
636 in precursor protein import into the chloroplasts of *Arabidopsis thaliana*. **Plant, cell & environment**
637 36: 970-983
638 Sun F, Carrie C, Law S, Murcha MW, Zhang R, Law YS, Suen PK, Whelan J, Lim BL (2012) AtPAP2 is a tail-
639 anchored protein in the outer membrane of chloroplasts and mitochondria. **Plant signaling &**
640 **behavior** 7: 927-932
641 Tsutsui H, Higashiyama T (2017) pKAMA-ITACHI vectors for highly efficient CRISPR/Cas9-mediated
642 gene knockout in *Arabidopsis thaliana*. **Plant & cell physiology** 58: 46-56
643 VanderLinden RT, Hemmis CW, Yao T, Robinson H, Hill CP (2017) Structure and energetics of pairwise
644 interactions between proteasome subunits RPN2, RPN13, and ubiquitin clarify a substrate recruitment

645 mechanism. **J Biol Chem** 292: 9493-9504
646 Voon CP, Law YS, Guan X, Lim SL, Xu Z, Chu WT, Zhang R, Sun F, Labs M, Leister D, Pribil M, Hronkova
647 M, Kubasek J, Cui Y, Jiang L, Tsuyama M, Gardestrom P, Tikkanen M, Lim BL (2021) Modulating the
648 activities of chloroplasts and mitochondria promotes ATP production and plant growth. **Quantitative**
649 **Plant Biology** 2: 1-10
650 Wang Q, Liu Y, Soetandyo N, Baek K, Hegde R, Ye Y (2011) A ubiquitin ligase-associated chaperone
651 holdase maintains polypeptides in soluble states for proteasome degradation. **Mol Cell** 42: 758-770
652 Wu X, Li L, Jiang H (2016) Doa1 targets ubiquitinated substrates for mitochondria-associated
653 degradation. **The Journal of cell biology** 213: 49-63
654 Yoo SD, Cho YH, Sheen J (2007) Arabidopsis mesophyll protoplasts: a versatile cell system for transient
655 gene expression analysis. **Nat Protoc** 2: 1565-1572
656 Zhang R, Guan X, Law YS, Sun F, Chen S, Wong KB, Lim BL (2016) AtPAP2 modulates the import of the
657 small subunit of Rubisco into chloroplasts. **Plant signaling & behavior** 11: e1239687
658 Zhang T, Ye Y (2016) Doa1 is a MAD adaptor for Cdc48. **The Journal of cell biology** 213: 7-9
659 Zheng J, Li L, Jiang H (2019) Molecular pathways of mitochondrial outer membrane protein
660 degradation. **Biochemical Society transactions** 47: 1437-1447
661

662

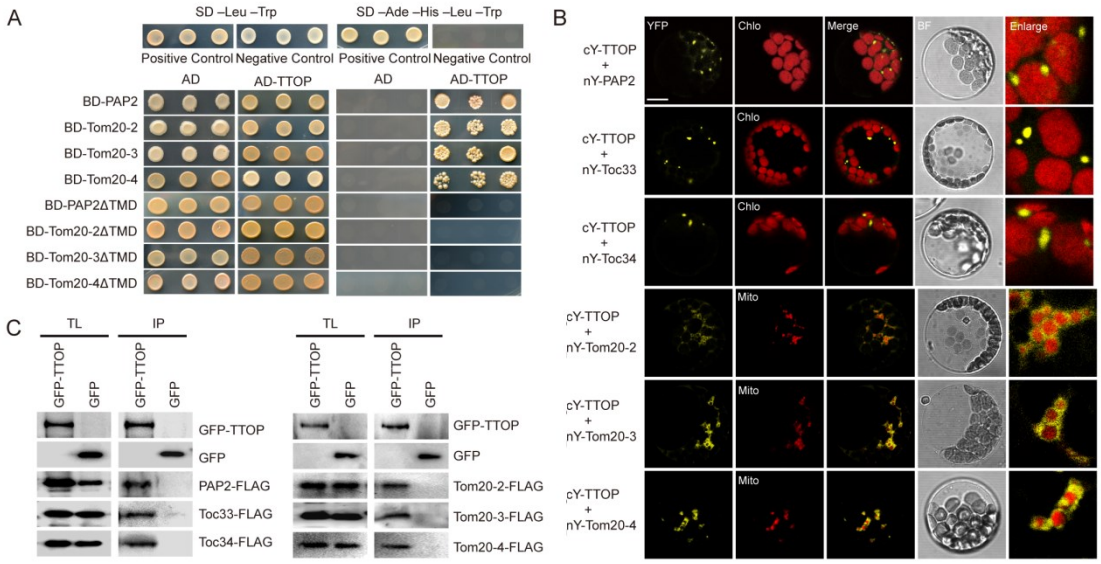

Figure 1. TTOP interacts with chloroplast and mitochondrial outer membrane tail-anchored proteins.

(A) Yeast two-hybrid analysis of the interaction between TTOP and tail-anchored (TA) proteins. Yeast from the Y2HGold strain were co-transformed with pairs of the indicated constructs encoding TTOP and full-length or TMD-truncated (ΔTMD) TA proteins. The TMD-truncated TA proteins include PAP2ΔTMD (a.a. 1-614 & 637-656), Tom20-2ΔTMD (a.a. 1-182 & 201-210), Tom20-3ΔTMD (a.a. 1-174 & 193-202), and Tom20-4ΔTMD (a.a. 1-161 & 179-187). Co-transformation of pGADT7-T and pGBKT7-53 constructs, or pGADT7-T and pGBKT7-lam constructs, into yeast was employed as the positive and negative controls, respectively. **(B)** Bimolecular fluorescence complementation (BiFC) analysis of the interaction between TTOP and TA proteins. Protoplasts were transiently co-transfected with the indicated pairs of constructs, which encode the fusion proteins carrying complementary N- or C-terminal YFP fragments (nY or cY), respectively. Reconstitution of YFP fluorescence in protoplasts was detected by confocal microscopy; representative images are shown. Chlo, chloroplast autofluorescence. Mito, mitochondria marked with MitoTracker. BF, brightfield. Scale bar, 10 μm. **(C)** Co-immunoprecipitation (co-IP) of TA proteins in **(B)** by TTOP from protoplast extracts. Protoplasts were transiently co-transfected with constructs encoding FLAG-tagged TA proteins and GFP-TTOP or GFP. Protoplast total lysis (TL) and immunoprecipitates (IP) eluted from GFP-Trap agarose were subjected to immunoblotting analysis with anti-GFP and anti-FLAG antibodies, respectively.

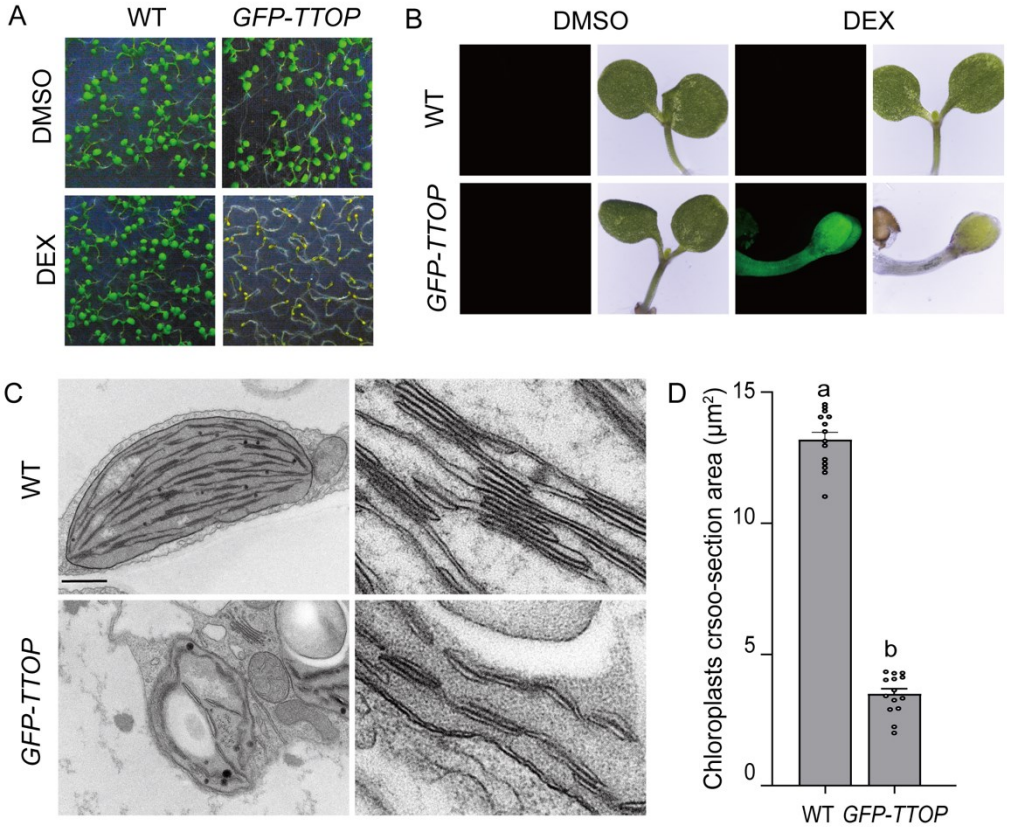

Figure 2. Overexpression of *TTOP* impairs chloroplast development.

(A and **B)** Col-0 **(**WT) and pTA7002-*GFP-TTOP* seedlings were germinated on half-strength MS medium containing 10 μM DEX or DMSO (mock control treatment lacking the inducer) for 7 days. Typical seedling phenotypes are shown in **(A)**. GFP fluorescence in seedlings was detected by CLSM; typical images are shown **(B)**. **(C)** TEM analysis of the ultrastructure of cotyledon chloroplasts in the DEX-treated seedlings in **(A)**. Left, representative TEM micrographs of chloroplasts; right, thylakoid development. (**D**) Micrographs were used to estimate the cross-sectional area (bar chart) occupied by chloroplasts with ImageJ software. Scale bar, 1.0 μm.

Bars show means ± SEM (n = 20 chloroplasts). Different letters indicate significant differences as analyzed by Tukey's HSD test ($P < 0.05$).

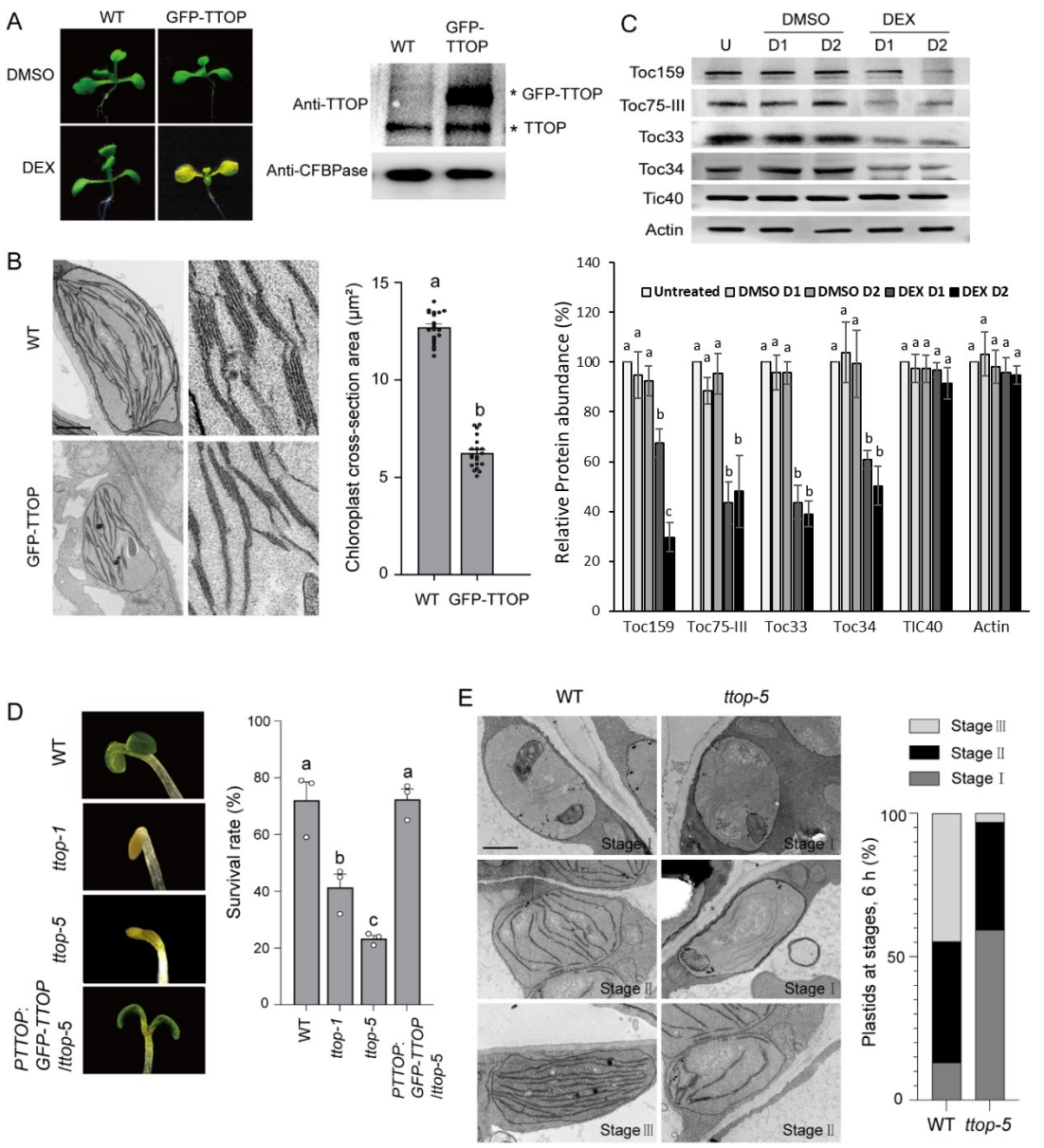

Figure 3. TTOP is essential for chloroplast biogenesis.

(A) Left, representative images of 5-day-old pTA7002-*GFP-TTOP* and wild-type Col-0 (WT) seedlings grown on half-strength MS medium after 3 days of growth on half-strength MS medium containing 10 μM DEX or DMSO. Right, DEX-induced accumulation of GFP-TTOP as revealed by immunoblotting with anti-TTOP antibodies. Anti-cFBPase was used as a loading control. **(B)** Transmission electron microscopy (TEM) analysis of the ultrastructure of chloroplasts in cotyledons of seedlings shown in **(A)**. Micrographs show chloroplasts (left) and thylakoid development (right). Scale bar, 1.0 μm. Bar chart shows estimates of chloroplast cross-sectional area determined from the micrographs using ImageJ software. **(C)** Immunoblotting analysis of TOC receptors in total leaf proteins from pTA7002-*GFP-TTOP* plants subjected to DEX or DMSO treatment for 1 (D1) or 2 days (D2), or untreated (U). Anti-actin was used as a loading control. Untreated samples = 100%. Band of untreated samples were normalized **(D)** Results of de-etiolation of *ttop-1*, *ttop-5*, *ttop-5 pTTOP:GFP-TTOP*, and WT seedlings, grown in the dark for 6 days, upon transfer into continuous light. After 2 days

711 of illumination, cotyledon phenotypes (left) and plant survival rates (right) were recorded. **(E)**
712 Left, TEM analysis of the ultrastructure of cotyledon plastids in different genotypes after 0, 6,
713 and 24 hours of illumination as in **(D)**. Right, proportions of plastids at each of three
714 developmental stages estimated after 6 hours of illumination. Scale bar, 1.0 μm. Bars show
715 means ± SEM (n = 20 chloroplasts in B, n = 3 experiments in C, $n \geq 30$ images in D, E).
716 Different letters indicate significant differences as analyzed by Tukey's HSD test ($P < 0.05$).

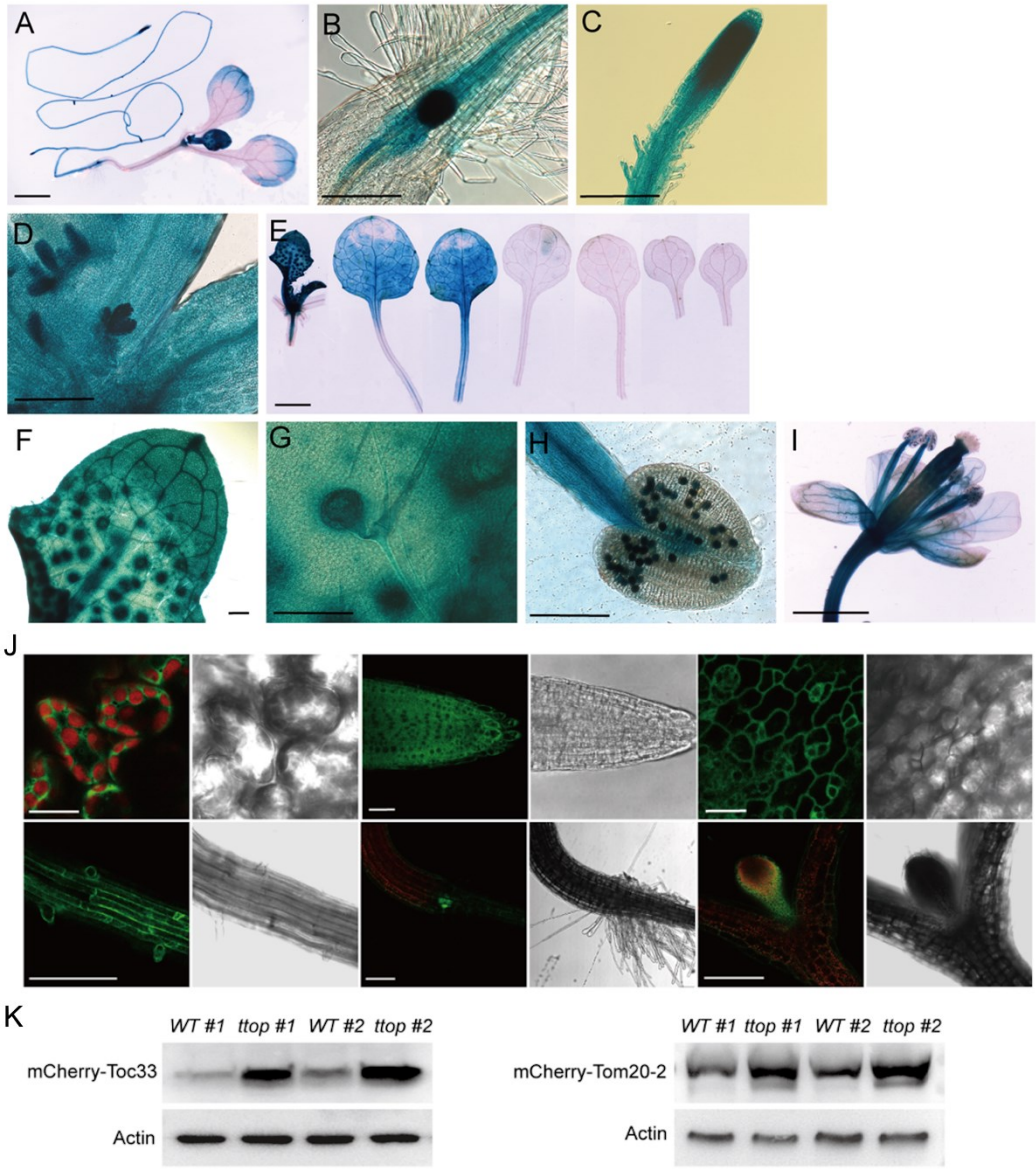

Figure 4. *In planta* expression patterns of TTOP.

Expression patterns of *TTOP* at different developmental stages in *pTTOP:GUS* plants. Ten-day-old seedlings **(A-D, F, G)** and 23-day-old plants **(E)** from *pTTOP:GUS* transgenic lines were used for GUS staining. Decreases in *TTOP* expression were observed in older tissues, particularly in leaves **(A, E)**, with high *TTOP* expression in newly grown leaves and no *TTOP* expression in fully grown leaves **(E;** left to right, youngest to oldest leaves**)**. High *TTOP* expression was also observed in meristematic regions, including the root-hypocotyl junction **(B)**, root meristem **(C)**, and shoot meristem **(D)**, and in other tissues such as trichome bases **(F** and **G)**, mature pollen **(H)**, and flowers **(I).** Scale bar in A, E, I, 2.0 mm. Scale bar in B, C, D, F, G, H, 200 µm. (**J)** Tissue expression pattern and subcellular localization of TTOP in 6-day-old *ttop-5 pTTOP:GFP-TTOP* transgenic seedlings. TTOP accumulates in mesophyll cells, roots, and epidermis. TTOP has a cytosolic localization in different tissues. Red signal is chlorophyll autofluorescence. Brightfield images are shown for reference. Scale bar in the upper panels, 20 µm. Scale bar in the below panels, 200 µm. **(K)** Transgenic *ttop-5* mutant plants expressing mCherry-Toc33 or mCherry-Tom20-2 were crossed with WT plants to obtain

WT plants expressing mCherry-Toc33 or mCherry-Tom20-2 for comparisons of mCherry-Toc33 or mCherry-Tom20-2 abundance between *ttop-5* and WT. Two individual homozygous lines for each *ttop* and WT genotype were tested by immunoblotting with anti-mCherry antibodies, which showed more mCherry-Toc33 and mCherry-Tom20-2 in the *ttop-5* mutant than the WT. Anti-actin was used as a loading control.

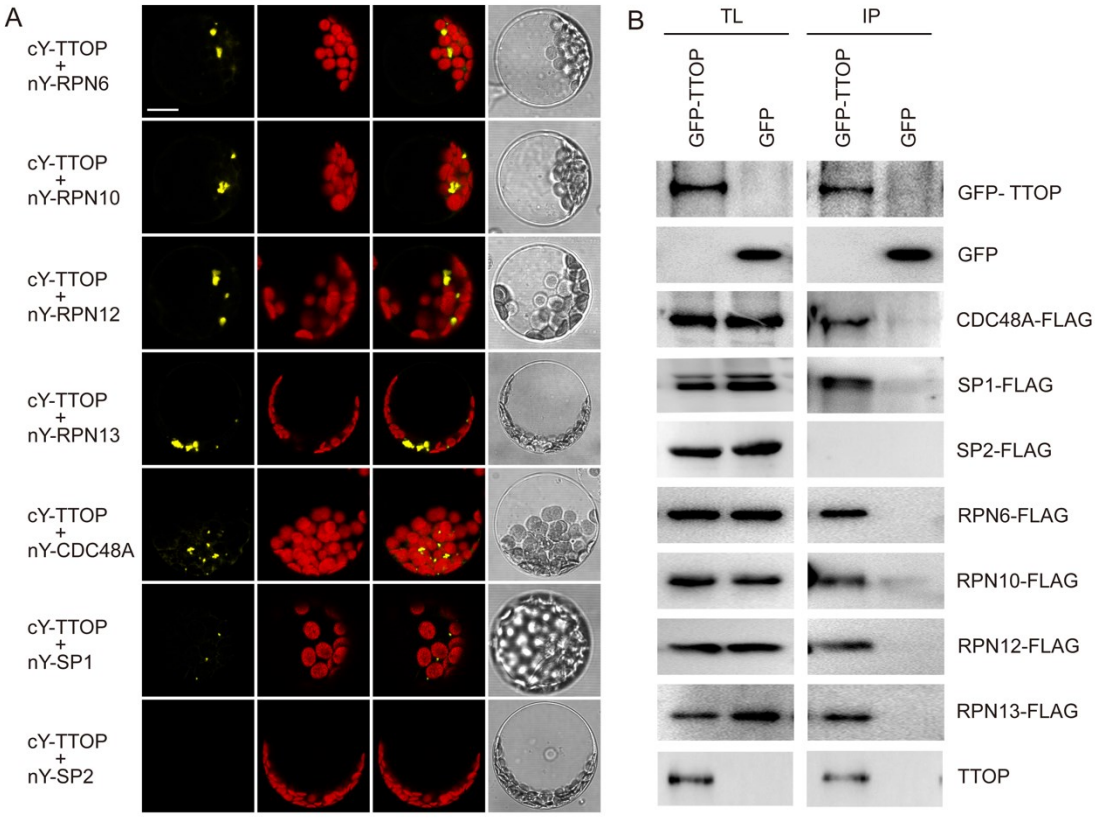

Figure 5. TTOP, chloroplast, and mitochondrial TA proteins, CDC48A, and 26S proteasome subunits form complexes *in vivo*.

(A) BiFC analysis of the interactions between TTOP and CDC48A, SP1, SP2, and 26S proteasome subunits. Protoplasts were co-transfected with the indicated pairs of constructs encoding fusion proteins with cY or nY. Reconstitution of YFP fluorescence in protoplasts was detected by confocal microscopy. Chlo, chloroplast autofluorescence. BF, brightfield. Scale bar, 10 µm. **(B)** Co-IP of CDC48A, SP1, or 26S subunits with TTOP from protoplast extracts. Protoplasts were co-transfected with constructs encoding GFP-TTOP or GFP and constructs encoding FLAG-tagged CDC48A, SP1, or 26S proteasome subunits. Protoplast extracts and elution proteins from GFP-Trap agarose were subjected to immunoblotting analysis with anti-GFP and anti-FLAG antibodies as described above.

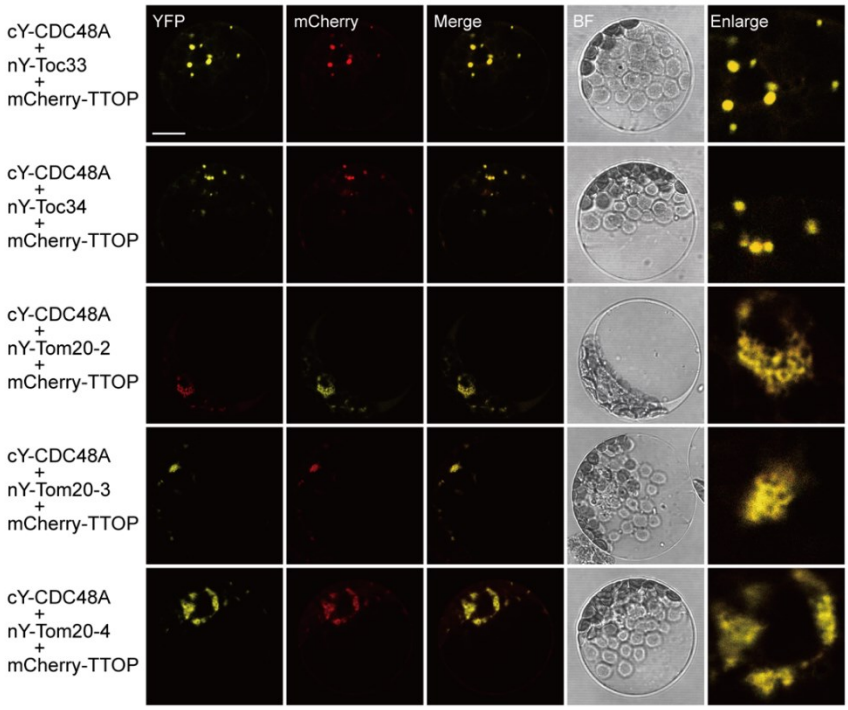

Figure 6. Co-localization of TTOP, CDC48A, and chloroplast or mitochondrial outer membrane TA receptors in protoplasts.

Protoplasts were co-transfected with constructs encoding TTOP fused to mCherry at its N terminus or encoding CDC48A and TA proteins fused to nY or cY at their N termini. YFP and mCherry fluorescence in protoplasts was analyzed by CLSM; representative confocal images are shown. Overlap of YFP and mCherry signals is shown in protoplasts, indicating the co-localization of TTOP and CDC48A with TA proteins. BF, brightfield. Scale bar, 10 μm.

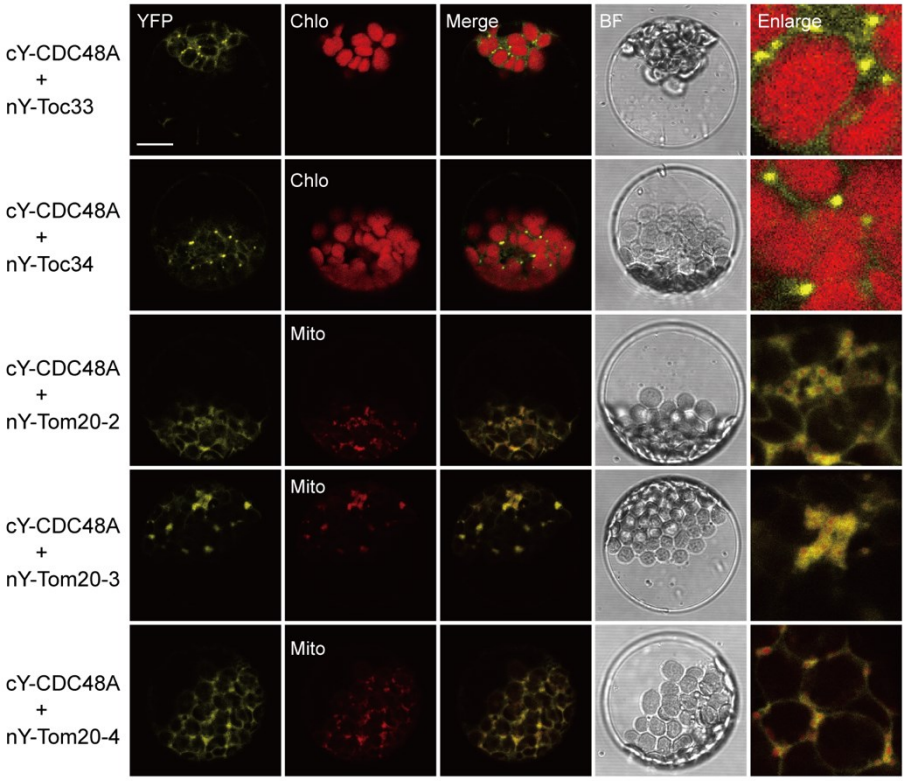

Figure 7. BiFC analysis of the interaction between CDC48A and the TA receptor proteins. Protoplasts were co-transfected with the indicated pairs of constructs encoding CDC48A or TA proteins carrying nY or cY in their respective N termini. Reconstitution of YFP fluorescence in protoplasts was detected by CLSM, and the representative confocal images are shown. Chlo, chloroplast auto-fluorescence; Mito, mitochondria marked with MitoTracker. BF, brightfield. Scale bar, 10 μm.

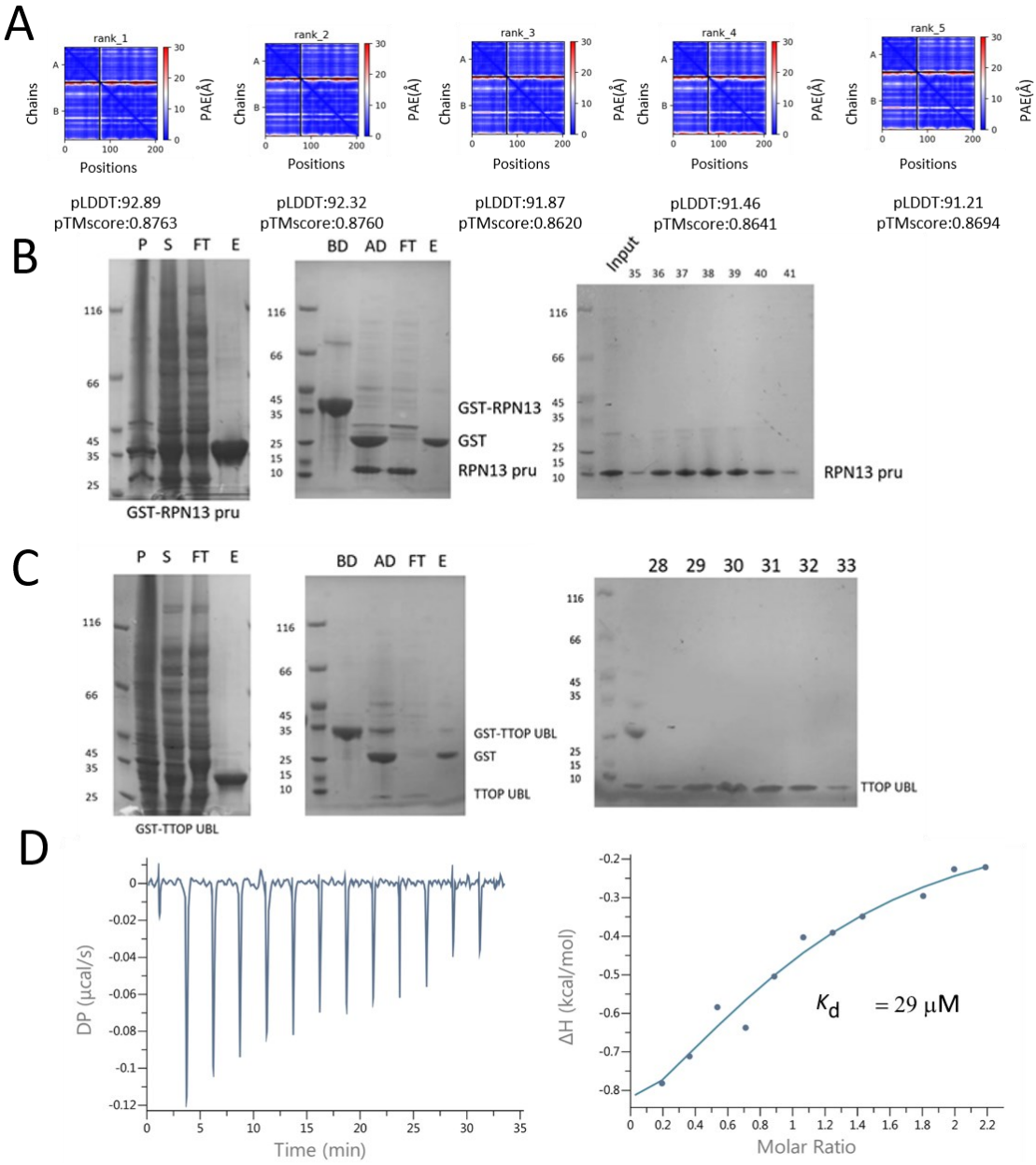

Figure 8. TTOP UBL domain could interact with RPN13 pru domain.

By AlphaFold2 prediction, the high value of pLDDT and pTMscore and the low value of PAE showed that TTOP UBL could interact with the pru domain of RPN13. Recombinant TTOP UBL domain (B) and RPN13 pru domain (C) were purified by using GST fusion protein purification, on-column digestion and HiLoad 26/200 Superdex 200pg column. Isothermal titration calorimetry (ITC)-based measurement of the binding affinity between the UBL domain of TTOP and the pru domain of RPN13 at a 1:1 ratio is determined to be 29μM (D).

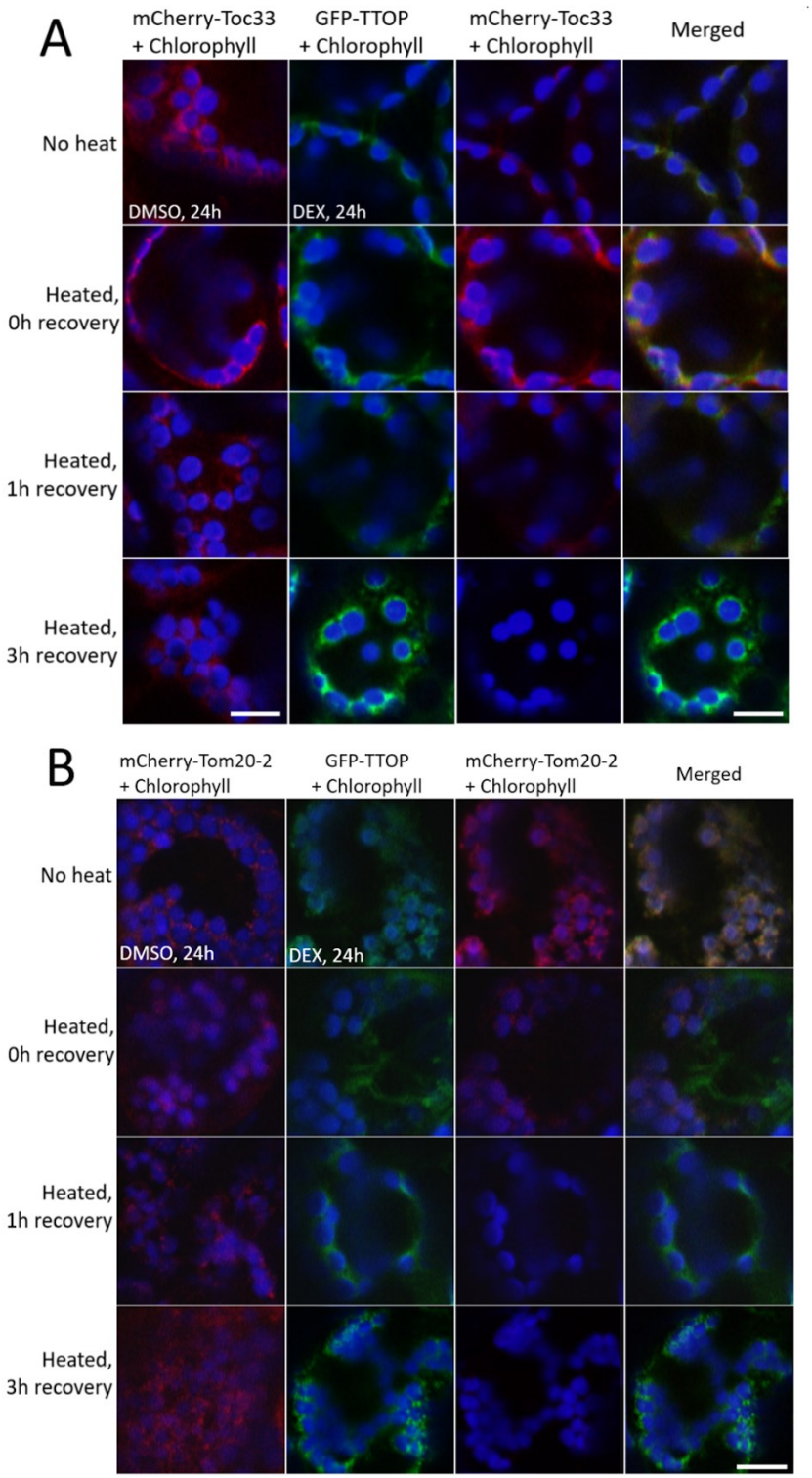

Figure 9. TTOP assists the degradation of Toc33 and Tom20-2 in planta.
The transgenic DEX-GFP-TTOP line was transformed with 35S: mCherry-Toc33 (A), and 35S: mCherry-Tom20-2 (B), respectively. 25μM DEX were sprayed to the seedlings at 8-day-old. Some seedlings were treated with DMSO as negative controls. After 24 h, seedlings were placed in 45°C incubator for 30 minutes (heated) or kept in R.T. (no heat). Heat-treated seedlings were allowed to recover in R.T. for 1 and 3 hours prior to the imaging. Green: GFP-PFP; Red: mCherry-Toc33; Blue: Chlorophyll auto-fluorescence. Bars = 20 μm.

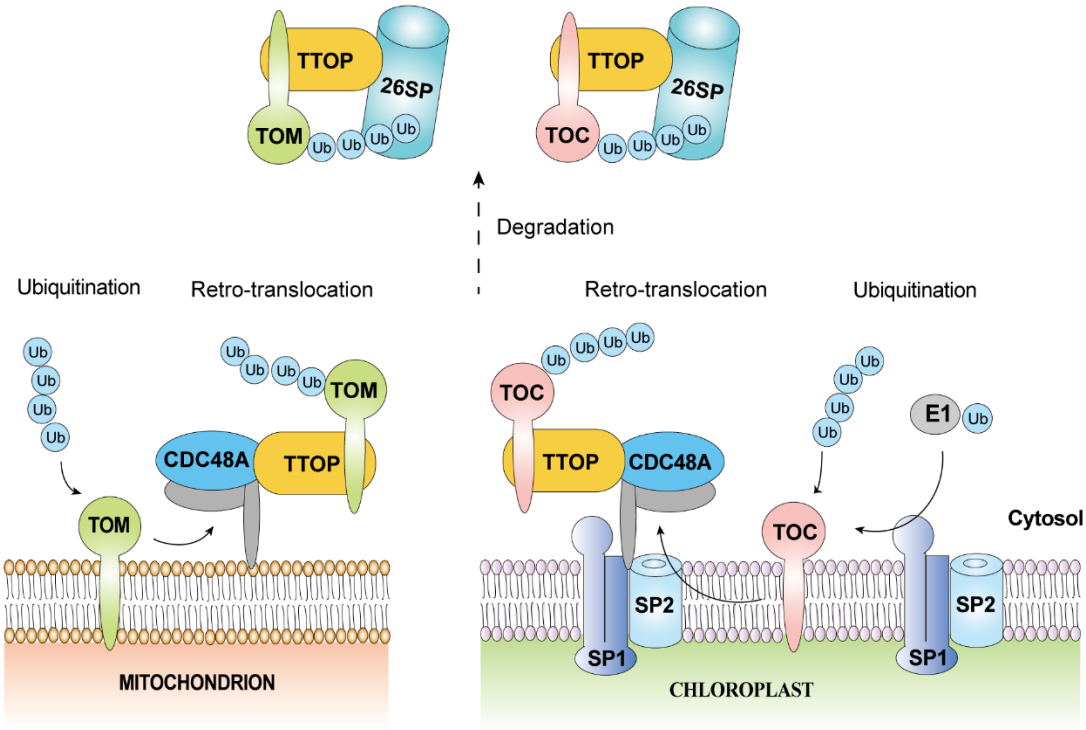

Figure 10. Proposed model for the role of TTOP in a converged pathway for the degradation of tail-anchored receptors of TOC and TOM translocases. In the CHLORAD proteolytic system, TOC components of the chloroplast protein import machinery are selectively removed by the SP1-SP2-CDC48A complex. After the TOC tail-anchored receptors are ubiquitinated by SP1, SP2 and CDC48A act as a conduit and a molecular motor, respectively, to mediate retrotranslocation of TOC complex out of the membrane. Similarly, tail-anchored receptors of TOM complexes are also ubiquitinated by an unknown E3 ubiquitin ligase and presumably pulled out from the outer envelope membrane (OEM) by CDC48A. Cytosolic TTOP then binds to the transmembrane domains (TMDs) of the retrotranslocated TOC/TOM receptors, masking the hydrophobic aggregation-prone TMDs and stabilizing ubquitinated TOC/TOM complexes in the cytosol. TTOP, via its interaction with RPN subunits of the 26S proteasome, then delivers the ubiquitinated receptors to the 26S proteasome for degradation. Association of TTOP with both CDC48A and RPN subunits of the 26S proteasome might allow efficient delivery of ubiquitinated receptors to the proteasome, thereby avoiding the risk of protein aggregation and enhancing degradation efficiency.